



## Study of the Effective Parameters on Selective Catalytic Reduction of NO<sub>x</sub> by Ammonia over a Vanadia-Titania Catalyst from Exhaust Gases

Hossein Atashi

Department of Chemical Engineering, Faculty of Engineering, University of Sistan & Baluchestan, P.O. Box 98164-161, Zahedan, Iran

atashi.h64.usb@gmail.com

Esmaeel Moradian\*

Email: \*moradian67@gmail.com

### Abstract

The removal of nitrogen oxides (NO<sub>x</sub>) is crucial problem for global environment. In This study, a 3D dynamic simulation model for the application in investigation of the reaction characteristic and the phenomena of transport in the catalytic filter of the SCR reactor is introduced. In order to make an assessment on the kinetic parameters of the model by the mechanism of Eley-Rideal (ER) from experimental data, an optimization method which acts by integrating the Taguchi method, a real-coded genetic algorithm auxiliary model is proposed. With the aid of the introduced dynamic model, the impacts of the key parameters, namely operating temperature, the gas hourly space velocity, the amount of the applied ammonium and the cross section of the channel of SCR reactor on the NO<sub>x</sub> conversion and NH<sub>3</sub> slip phenomena were investigated. By comparing with the experimental data available in the literature, it was validated and it is found that NO<sub>x</sub> conversion increases with the decrease in the operation temperature, the space velocity, the concentration of H<sub>2</sub>O, the ratio of NH<sub>3</sub>/NO<sub>x</sub>, and the increase in O<sub>2</sub> concentration. Moreover, it is evident that the reactors with the square shaped cross section have more percentage of conversion but the resident time in the corner increased.

**Keywords:** DeNO<sub>x</sub>; SCR reactor; V<sub>2</sub>O<sub>5</sub>/TiO<sub>2</sub>; Optimal design.

# Council for Innovative Research

Peer Review Research Publishing System

**Journal:** Journal of Advances in Chemistry

Vol. 6, No. 2

editor@cirworld.com

[www.cirworld.com](http://www.cirworld.com), [member.cirworld.com](http://member.cirworld.com)

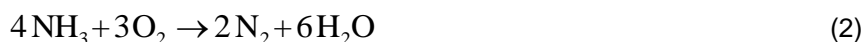
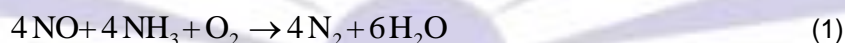


## Introduction

The gaseous pollutants and particles elimination in gases at high temperature which is required in the thermal power plants has always been a crucial environmental concern. Nowadays, while the NO<sub>x</sub> emission regulation has become more and more strict, much effort has been concentrated on the development of the technology of the efficient NO<sub>x</sub> control (DeNO<sub>x</sub>) [1-3]. Among various methods, the process of selective catalyst reduction (SCR) is one of the techniques widely applied in NO<sub>x</sub> elimination from flue gases at about 250-500 °C. The system of SCR in which urea or NH<sub>3</sub> are serving as a reductant, is often considered as one of the highly potential and effective technologies in accordance with NO<sub>x</sub> emission regulation of the euro V and VI standards for the heavy duty diesel engines[4-7].

Many studies have been conducted on numerous metal oxide catalysts, such as MoO<sub>3</sub>/TiO<sub>2</sub>, V<sub>2</sub>O<sub>5</sub>/TiO<sub>2</sub> and CuO/Al<sub>2</sub>O<sub>3</sub>, for NO elimination [8-9]. However, the fact is that in order to avoid the deactivation by SO<sub>2</sub> and H<sub>2</sub>O which takes place at low temperatures [10], these catalysts usually function at high temperatures (higher than 350 °C). Also, Fe zeolite SCR catalysts which are commercially available for stationary applications is shown to operate at temperature up to 600 °C. Fe zeolite SCR when exposed to high temperatures in the presence of H<sub>2</sub>O, may be subjected to the problems of stability. When exposed to the temperatures higher than 600 °C, in a process flow with high concentration of H<sub>2</sub>O, zeolites SCR has the tendency to be deactivated by de-alumination, while the Al<sup>3+</sup> ions in the SiO<sub>2</sub>-Al<sub>2</sub>O<sub>3</sub> framework start to migrate out of the structure, the Cu/zsm-5 plays an active role in NO<sub>x</sub> reduction within the temperature window of about 200-400 °C, but its thermal durability is insufficient [11]. It is evident that the V<sub>2</sub>O<sub>5</sub> catalyst shows quite high activity for NO elimination at low temperatures, and the presented SO<sub>2</sub> in the flue gas does not deactivate the V<sub>2</sub>O<sub>5</sub> catalyst but even can enhance its activity in the absence of H<sub>2</sub>O [12]. Therefore, it seems that the V<sub>2</sub>O<sub>5</sub> catalyst could be an excellent alternative for SCR of NO with NH<sub>3</sub>. The vastly studied support for vanadium is TiO<sub>2</sub> as it is resistance to poisoning effects of sulfur and has the ability to effectively disperse the V<sub>2</sub>O<sub>5</sub>. But, Titania dose suffer from several limitations, such as it is expensive, sintering non-resistance, and has relatively low surface area [13, 14]. Mixed oxides containing both TiO<sub>2</sub> and Al<sub>2</sub>O<sub>3</sub> have also been examined extensively by Centi et al. [15]. It was shown that Al<sub>2</sub>O<sub>3</sub> component (with no addition of CuO to the catalyst) attracts the sulfate species which are generated and originally formed at the surface of vanadia, and as a result, this shields the active sites of vanadium. The structure of the surface of vanadyl species present in catalysts shown to have a prominent impact on the activity and the selectivity in the NO<sub>x</sub> reduction by ammonia.

SCR systems are capable of the selective reduction of NO and NO<sub>2</sub> even in the O<sub>2</sub> abundant environments, which is usually encountered in the exhaust gases of diesel motors. Anyway, such SCR systems adjustment for the practical applications needs to optimize some of the different parameters such as the position of the SCR catalyst, the space velocity, the strategy of the injection of urea. In order to make an assessment on the performance of DeNO<sub>x</sub>, studies were conducted by Gieshoff et al. [16], in which the parameters such as the NH<sub>3</sub>/NO<sub>x</sub> and the NO<sub>2</sub>/NO<sub>x</sub> ratios over a V<sub>2</sub>O<sub>5</sub> SCR catalysts were varied. For the purpose of enhancement in the NO<sub>x</sub> conversion efficiency, some studies have been carried out by the use of the common parameters in diesel engine, at different raw NO<sub>x</sub> emission levels [17]; for example space velocity, the SCR catalyst temperature, and the oxidation catalyst volume. In addition, several dynamic investigations on the V<sub>2</sub>O<sub>5</sub> SCR catalyst have been conducted with the help of a kinetic model, which has a supportive role of an Eley-Rideal (ER) mechanism for the reactions of SCR. Measurements of the kinetics of SCR on vanadium oxide supported on carbon-ceramic catalyst in the absence of both SO<sub>2</sub> and H<sub>2</sub>O was performed by Valdes-Solis et al. [18], it was found that it showed the Langmuir-Hinshelwood mechanism. In contrast, Hsu and Teng [19] had made a different conclusion in which the redox mechanism (i.e. the Mars-van Krevelen model) showed a more justified correlation of experimental data than the Langmuir-Hinshelwood mechanism and Eley-Rideal mechanism, the research group [20] studied the kinetics in the absence of H<sub>2</sub>O but after a pre-sulfated step, and concluded that rather than the Langmuir-Hinshelwood or redox mechanism, the Eley-Rideal mechanism could be the most appropriate mechanism for description of the SCR of NO with NH<sub>3</sub> over V<sub>2</sub>O<sub>5</sub>/TiO<sub>2</sub> catalyst. The reaction of SCR takes place in accordance with the following stoichiometry:



Here, in a solid-catalytic reaction, the selective reduction of NO<sub>x</sub> is made by NH<sub>3</sub>, typically in the structures of the low pressure drop honeycomb V<sub>2</sub>O<sub>5</sub>/TiO<sub>2</sub>. It can be seen that the NO is reduced according to (1), and at the same time the amount of a parallel NH<sub>3</sub> oxidation by O<sub>2</sub> (2) must be minimized. Regardless to the type of catalyst, the shape & characteristics of reactors such as the cross section of channels can have a great impact on the amount of the conversion. In addition, the state of cost-effectiveness or feasibility of construction of such a reactor with desirable characters must be noted. In this paper, just the cross section of channels is considered.

## 2 Experimental database

The experimental information of this model has been obtained from Due-hansen et al. [21]. In their study, they investigated the steady-state performance of vanadium-based honeycomb monolith catalysts in the SCR for elimination of NO with the help of the NH<sub>3</sub>. In the current model, some conditions were considered for example the concentration of NO was maintained at 1000ppm and the space velocity was fixed at 8,000h<sup>-1</sup>. According to the optimized experimental results

of Due-hansen et al. [21], the inlet concentration of ammonia and the inlet oxygen concentration were set to 11000 ppm and 3.5%, respectively. Optimum  $\text{NO}_x$  conversion was obtained at 523 K. Table 1 depicts the detailed characteristics of catalyst and its operating conditions which was employed for the study. In which, the concentrations of various components such as  $\text{NO}$ ,  $\text{NO}_2$ ,  $\text{N}_2\text{O}$ ,  $\text{NH}_3$ ,  $\text{H}_2\text{O}$ ,  $\text{O}_2$  and  $\text{HNO}_3$  were altered in order to find their influence on the SCR functionality. Here, the properties of  $\text{NO}$  conversion with respect to temperature were measured similar to data in Fig 3.

### 3 Mathematical model for an SCR reactor

In the following, an isothermal pseudo-homogeneous model is developed which results in the differential equations based on unsteady state continuity equations. The SCR reaction system is illustrated in Fig. 1, where  $\text{NH}_3$  is applied as a reducing agent in  $\text{NO}$  reduction. Before entering to the catalyzed bed, first,  $\text{NO}$  is diluted with  $\text{N}_2$  and  $\text{O}_2$  and then mixed with the  $\text{NH}_3$  reacting agent. In the following subsections, the reaction kinetics mechanisms and the phenomena of transport in the SCR reactor are explained and formulated.

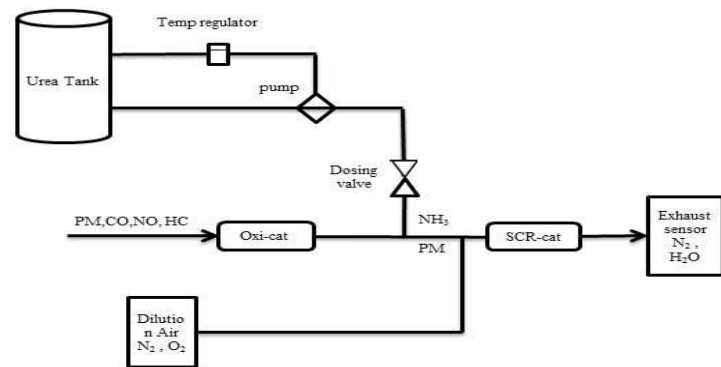


Figure 1 The SCR system for reduction of NO

#### 3.1 kinetics model

The reactions of (1) and (2) describe the mechanism of the  $\text{NO}$  reduction reaction with the application of  $\text{NH}_3$  over catalyst in which the rates of reaction are given by [4]:

$$r_1 = k_1 C_{\text{NO}} \frac{a C_{\text{NH}_3}}{1 + a C_{\text{NH}_3}} \quad (3)$$

$$r_2 = k_2 C_{\text{NH}_3} \quad (4)$$

In the above equations, it is assumed that the reaction constants obey the Arrhenius law as follows:

$$k_i = A_i \exp\left(-\frac{E_i}{R_g T}\right) \quad (5)$$

$$a = A_0 \exp\left(-\frac{E_0}{R_g T}\right) \quad (6)$$

In which  $E_i$  represents the activated energy (J/mol),  $R_g$  indicates the gas constant (J/ mol K) and  $T$  is the temperature (K).

#### 3.2 The equations of transport in the SCR reactor

Two main portions comprise the SCR reactor: the portion of free channel and the portion of catalyzed-bed where the reaction takes place. In the followings, the transport phenomena through individual part are discussed:



The Navier-Stokes equations describe the flow in the free channel:

$$\rho \frac{\partial \mathbf{u}}{\partial t} + \rho(\mathbf{u} \cdot \nabla) \mathbf{u} = \nabla \cdot \left[ -P \mathbf{I} + \eta(\nabla \mathbf{u}) + (\nabla \mathbf{u})^T - \left( \frac{2\eta}{3} \right) (\nabla \cdot \mathbf{u}) \mathbf{I} \right] \quad (7)$$

$$\frac{\partial \rho}{\partial t} + \nabla \cdot (\rho \mathbf{u}) = 0 \quad (8)$$

It worth noting that Eq. (7) describes the slightly compressible behavior due to the gas flow, and Eq. (8) is the equation of continuity. Where  $\rho$  shows the density ( $\text{kg/m}^3$ ),  $\mathbf{u}$  is the velocity (m/s),  $\eta$  indicates the viscosity ( $\text{kg}/(\text{m} \cdot \text{s})$ ), and  $p$  denotes the pressure (Pa). In the case of the porous domain, the Brinkman equations explain the flow [22]:

$$\left( \frac{\rho}{\varepsilon_P} \right) \frac{\partial \mathbf{u}}{\partial t} + \left( \frac{\eta}{\kappa} + Q \right) \mathbf{u} = \nabla \cdot \left[ -P \mathbf{I} + \left( \frac{1}{\varepsilon_P} \right) \left\{ \eta(\nabla \mathbf{u}) + (\nabla \mathbf{u})^T - \left( \frac{2\eta}{3} \right) (\nabla \cdot \mathbf{u}) \mathbf{I} \right\} \right] \quad (9)$$

$$\frac{\partial(\varepsilon_P \rho)}{\partial t} + \nabla \cdot (\rho \mathbf{u}) = 0 \quad (10)$$

Where  $\varepsilon_p$  represents the porosity (dimensionless) and  $k$  is the permeability ( $\text{m}^2$ ) of the porous medium. As it can be seen in (7) and (9), the momentum-balance equations are tightly related. The term on the left-hand side of the Navier-Stokes equation corresponds to the transported momentum by convection in free flow. In the Brinkman formulism, this term is substituted by a contribution related to the drag force experienced by the fluid as it flows through a porous medium.

**Table 1 The physical properties of the SCR reactor and operating condition**

Parameters	Value	Units	Name
C <sub>NO</sub>	1000	ppm	Inlet NO concentration
L	0.36	m	Length of reactor
r	0.1	m	Radius of reactor
r <sub>c</sub>	0.8	m	Radius of catalyzed bed
u	0.046	m/s	Inlet velocity
NH <sub>3</sub> /NO	1.1	-	Ratio of NH <sub>3</sub> to NO
a <sub>s</sub>	60	m <sup>2</sup> g <sup>-1</sup>	Specific surface area
e <sub>p</sub>	0.4	-	porosity
κ	1e-7	m <sup>2</sup>	permeability
R <sub>g</sub>	8.3141	J/molk	Gas constant
P	101.325	pa	pressure
T	523	k	Temperture
GHSV	8000	h <sup>-1</sup>	Gas hourly space velocity
V <sub>2</sub> O <sub>5</sub>	3	wt %	V <sub>2</sub> O <sub>5</sub> content
F	300	Nml/min	Total flow
m	48000	#	Number of mesh

The boundary conditions include:

$$\mathbf{u} \cdot \mathbf{n} = v_0 \quad \text{inlet}$$

$$\mathbf{u} = \mathbf{0} \quad \text{walls}$$

$$\mathbf{p} = \mathbf{p}_{\text{ref}} \quad \text{outlet}$$

The viscous stresses are neglected at the outlet, and the pressure is adjusted at 1 atmosphere. It must be reminded that the Brinkman equation is a generalization form of Darcy's law whose aim is to facilitate the boundary conditions matching at the interface between the catalyst larger pores and the permeable medium. The diffusion-convection equations at unsteady state are utilized for the description of the mass-balance equations:

$$\frac{\partial C_i}{\partial t} + \nabla \cdot (-D \nabla C_i + \mathbf{u} C_i) = R_i, \quad i = \text{NO, NH}_3, \text{O}_2, \text{N}_2 \text{ and H}_2\text{O} \quad (11)$$

Where  $D_i$  is the representative of diffusion coefficient ( $\text{m}^2/\text{s}$ ),  $c_i$  indicates the concentration of species, and  $\mathbf{u}$  denotes the velocity vector ( $\text{m/s}$ ). The term  $R_i$  is associated to the net rate of reaction for each of the species, which is a function of the reaction rates, (1) and (2), and also the reaction stoichiometry. In the free channel, the inlet conditions are equal to the inlet concentrations; and in the case of the outlet, as the diffusion coefficient and the viscosity of gas are dependent to the temperature and pressure, the convective flux condition is applied, the used corrections are mentioned in continue

$$D = 2.695 \times 10^{-3} \frac{\sqrt{T^3 (M_i + M_o) / (2 \times 10^3 M_i M_o)}}{P \sigma_i \sigma_o \Omega_D} \quad (12)$$

$$\eta = 2.699 \times 10^{-6} \frac{\sqrt{T (1 \times 10^3 M)}}{\sigma^2 \Omega_V} \quad (13)$$

In which  $M_i$  and  $M_o$  correspond to the molar mass ( $\text{kg/mol}$ ), and  $\sigma_i$  and  $\sigma_o$  denote the diameters ( $\text{m}$ ) of the gas species. In addition,  $p$  indicates the pressure ( $\text{Pa}$ ) and  $\Omega_D$  and  $\Omega_V$  are representatives of collision integrals [23].

In Table 1, the nominal operating condition and the physical characteristics of the SCR reacting system are mentioned. In this account, it must be highlighted that the proposed 3-Dimensional dynamic model, which is relatively different from the previous one- and two-dimensional steady-state models of monolith reactors [24], can make it easier to investigate the phenomena of the interior transport via porous catalyst and the spatial concentration distribution in the SCR reactors.

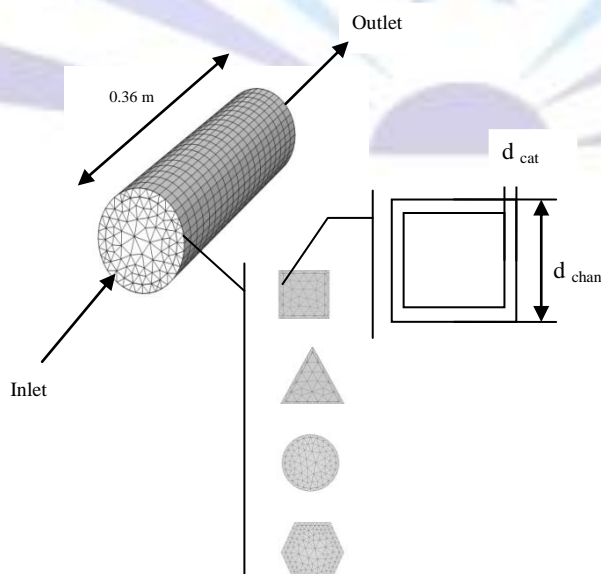
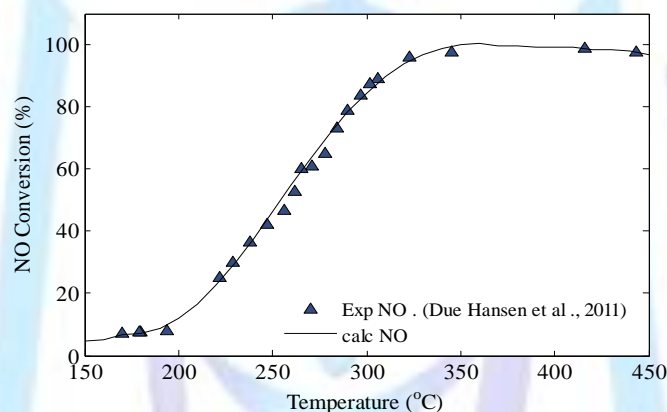


Figure 2 The schematic graf of the SCR reactor with various cross section

In the resented article, in order to simulate the 3D dynamic behavior of the SCR, finite element software is employed. In the following simulation studies, the fine mesh and Direct (mumps) solver with time step of 0.1 s are utilized and the error control of relative tolerance of  $1 \times 10^{-5}$  and absolute tolerance of  $1 \times 10^{-7}$  are considered. The mesh grid of the formulated 3D model is illustrated in Fig. 2. For the purpose of the PDE model parameters estimation such as activated energies, constants of the reaction rate and frequency constants, an optimization algorithm is introduced. Due to the possibility of the direct operation over real numbers and no need to the encoding and decoding procedures, the use of the real-coded genetic algorithm (RCGA) seems to be easier. Moreover, the RCGA has showed to benefit from the high efficiency and accuracy for optimization of the process. For application of the real-coded genetic algorithm (RCGA) [25] for the SCR

model, the objective function was set as  $\phi = \sum_{m=1}^n (X_{NO_{calc_m}} - X_{NO_{exp_m}})^2$  in which  $X_{NO_{calc}}$  represents the output of the model, and  $X_{NO_{exp}}$ , which corresponds to the experimental data, both are adopted from Due-hansen[21], before going through the optimization procedure. With setting the RCGA parameters as  $N = 200$  (population number),  $P_r = 0.2$  (possibility of reproduction) and  $G = 100$  (number of generations).

Fig. 3 and Table 2 depict the results of the fitting procedure. Calculated values of NO conversion show good accordance with the experimental data. The values of E1 and E2 were set in the ranges of published values (57 -65 and 81 -87 kJ/mol, respectively, both in [26-27]). Also the constants of the reaction rate are confined in the range of  $0.7 \times 10^6 \leq k_1 \leq 1.3 \times 10^6$ ,  $6.7 \times 10^7 \leq k_2 \leq 9 \times 10^7$ .



**Figure 3** Result of fitting in model validation, experimental data from  $3V_2O_5/TiO_2$ , NO conversion(%) vs . operating temperature (k),  $y_{NO}=1000ppm, y_{NH_3}=1100ppm, y_{O_2}=3.5 \text{ vol}\%, y_{H_2O}=2.7 \text{ vol}\%, GHSV=8000 \text{ h}^{-1}, u=0.046 \text{ m.s}^{-1}$

**Table 2** Estimated parameter values in rate equations

Kinetic parameter	Estimated value	Unit
$k_1$	$9.97 \times 10^6$	$s^{-1}$
$k_2$	$7.68 \times 10^7$	$s^{-1}$
$E_1$	$5.76 \times 10^4$	J/mol
$E_2$	$8.42 \times 10^4$	J/mol
$A_0$	$2.67 \times 10^{-17}$	$m^3/mol$
$E_0$	$-2.35 \times 10^5$	J/mol
$\Phi$	$2.64 \times 10^{-2}$	-

The analysis of the kinetic for the individual SCR rate approaches was carried out for a various exhaust conditions. In continue, a comprehensive analysis is done with the aim of the determination of the effects the various parameters such as the temperature, the space velocities, and the concentration of  $O_2$ ,  $H_2O$ ,  $NO_2$ , and  $NH_3$ , on the efficiency of  $NO_x$  conversion over an SCR De $NO_x$  catalyst of the heavy duty diesel exhaust gases.

### 3.3 Effect of temperature

Only at specific temperatures, the surface reaction of  $NO_x$  reduction is effective. Hence, the simulations were carried out for five exits, in order to find out the specific range at which the reactions show effectiveness. The corresponding

temperature profiles of the temperatures 225°C, 250°C, 275°C, 300°C, & 325°C with the variation in the rate of molar flow and the temperatures are brought. In the case of a composite exhaust gas including 3.5% O<sub>2</sub>, 2.7% H<sub>2</sub>O, 1000 ppm NO, and 1100 ppm NH<sub>3</sub>, Fig 4 illustrates the comparison made between the flow rates of ammonia and nitrogen oxide (NO) along the length reactor. It can be clearly seen from the picture that, with the increase in the temperature of exhaust the reduction of NO shows enhancement. For instance, at a volume of 15 units, the NO levels are 10.85e-8 and 3.2e-8 (moles/sec), respectively, for the temperatures of 225 °C and 250 °C. Further increase in temperature does not result in the enhancement of NO reduction. by the analysis of the figure it can be concluded that, at a location of 15 volume units, the NO level is about 2.9 moles/sec. therefore, it can be concluded that in order to have the best reduction of NO with ammonia for the given NO emission level, the optimal temperature of the exhaust gas would be 250°C.

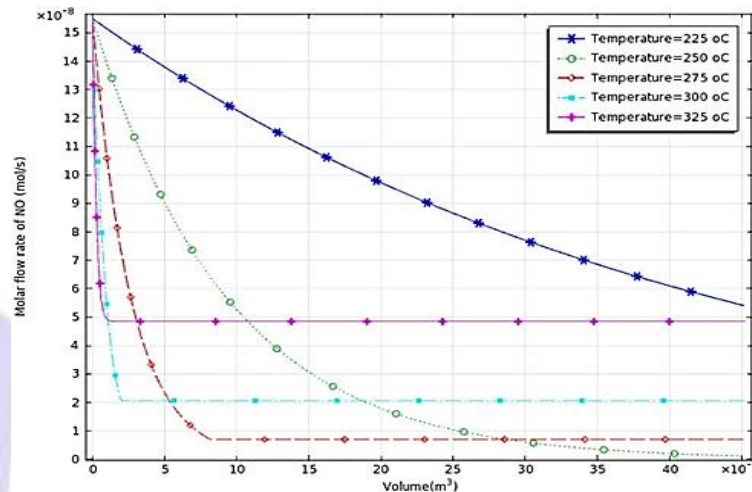


Figure 4 The effect of temperature on molar flow rate of NO (mol.s<sup>-1</sup>) under different volumes of SCR reactor.

### 3.4 Effect of space velocity

Before the performance of the optimum design, the influence of GHSV on the efficiency of the SCR reactor in NO elimination was investigated. In the case of heterogeneous fixed-bed catalysis which has a typical use in automobile after treatment, the residence time of the exhaust gases is defined in terms of the volumetric flow rate and the volume of the catalyst. The space velocity is equal to the volumetric gas flow rate at STP divided by the total volume of the catalyst, which is shown in continue:

$$GHSV = V_{\text{exhaust}} / V_{\text{catalyst}} \quad (14)$$

Here, GHSV is the abbreviation of the gas hourly space velocity in [1/h],  $V_{\text{exhaust}}$  corresponds to the volumetric flow rate of the exhaust gas in [m<sup>3</sup>/h], and  $V_{\text{catalyst}}$  indicates the catalyst's volume in [m<sup>3</sup>]. Since by reduction of the space velocity, the residence time of the exhaust gas increases, this leads to enhancement of the performance of the SCR DeNO<sub>x</sub>, but it may also result in various problems in the process of the vehicle installation. Also, since this method increased the volume of the catalyst, it may increase costs of production. The space velocity impact on the conversion of NO<sub>x</sub> for the composite exhaust gas which contains 3.5% O<sub>2</sub>, 2.7% H<sub>2</sub>O, 1000 ppm NO, and 1100 ppm NH<sub>3</sub> is depicted in Fig.5. As it can be clearly seen in Fig. 5, the SCR DeNO<sub>x</sub> performance shows a strong dependence on the space velocity. Especially, the light off temperature (LOT), in which the SCR DeNO<sub>x</sub> performance reaches to 55% conversion rate, shows an enhancement from 225 to 300 °C with the increase in the space velocity from 5,000 to 25,000 [1/h]. Moreover, it must be noted that at temperatures higher than 430 °C, the oxidizing property of NH<sub>3</sub> is more effective, and as a result, the SCR DeNO<sub>x</sub> performance slightly decreases. It is also observable that by reduction of the space velocities, NO<sub>x</sub> conversions increase. This is due to the fact that by increase in the space velocity, the residence time of the exhaust gas on the surface of the catalyst decreases [28].

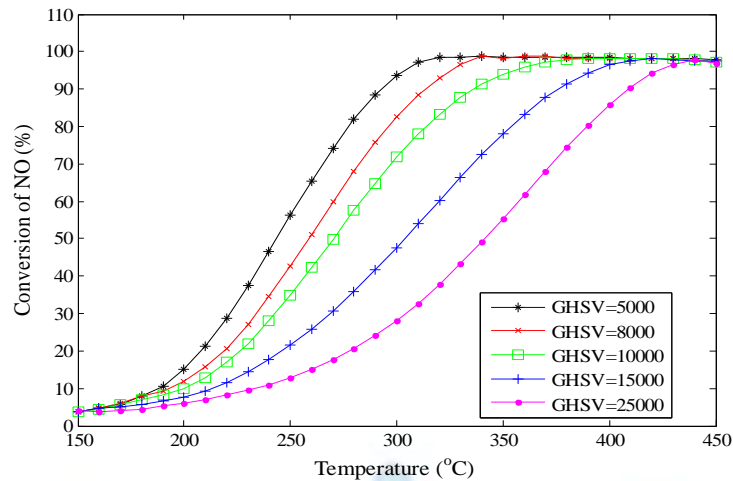


Figure 5 The effect of space velocity on the NO conversion(%) under different temperature.

### 3.5 Effect of the $\text{NH}_3/\text{NO}_x$ ratio

The emitted  $\text{NH}_3$  in the ambient air has the ability to react with sulfuric acid and nitric acid and form the salts of ammonium sulfate and ammonium nitrate, these compounds are important components of undesirable particulate matter [29]; also, they have an unpleasant odor. so, the amount of emitted  $\text{NH}_3$  normally is required to be less than 5-10 ppm. Fig. 6 shows the influence of  $\text{NH}_3/\text{NO}$  ratio on the NO reduction performance of the SCR reactor. In this study, the  $\text{NH}_3/\text{NO}_x$  ratio is varied from 0.5 to 1.3. In real vehicles, it is supposed that the test exhaust gas includes 2.7%  $\text{H}_2\text{O}$  and 3.5%  $\text{O}_2$  and has a space velocity of 8,000 [1/h]. In Fig. 6 the impact of the  $\text{NH}_3/\text{NO}_x$  ratio on the  $\text{NO}_x$  conversion when there is no  $\text{NO}_2$  (i.e., only the standard SCR reaction is taken into consideration) is illustrated. When the ratio of  $\text{NH}_3/\text{NO}_x$  is equal to 0.5, since the reductant  $\text{NH}_3$  is not enough for conversion of the exhaust NO into  $\text{N}_2$  through the standard reaction, the maximum  $\text{NO}_x$  conversion would be 45%, (Eq. (2)). By the increase of  $\text{NH}_3/\text{NO}_x$  ratio from 0.8 to 1.3, the conversion rate of  $\text{NO}_x$  into  $\text{N}_2$  reaches to 98%. However, when the operation temperature goes below 240 K the larger ratio of  $\text{NH}_3/\text{NO}$  leads to the more significant  $\text{NH}_3$  slip phenomenon this is due to the presence of excess  $\text{NH}_3$ .

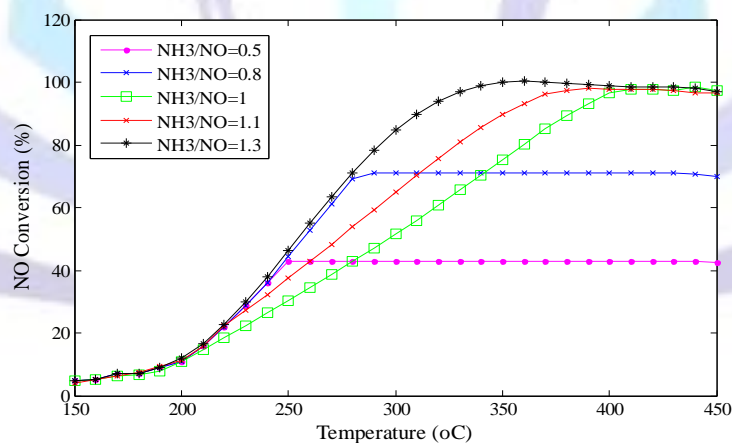


Figure 6 The effect of  $\text{NH}_3/\text{NO}$  ratio on NO conversion(%) under different temperature

### 3.6 Effect of $\text{H}_2\text{O}$ concentration

It is evident that the presence of  $\text{H}_2\text{O}$  leads to inhibition of some of the reactions in the process of SCR [30]. Despite the fact that the effect of  $\text{H}_2\text{O}$  is not directly associated to the SCR De $\text{NO}_x$  performance, the released heat of the exothermic process of adsorption, and as a result the absorbed heat in the desorption phase, may have a significant impact on the SCR catalyst. The  $\text{NO}_x$  conversion is studied at different temperatures and concentrations of  $\text{H}_2\text{O}$  in order to determine the influence of  $\text{H}_2\text{O}$  on the SCR performance. The results are shown in Fig. 4. For such simulation involves the assumption that the exhaust gas which includes 3.5%  $\text{O}_2$ , 1000 ppm NO, and 1100 ppm  $\text{NH}_3$  was fed into the SCR converter with the





space velocity of 8,000 [1/h]. It is observable that the  $\text{NO}_x$  conversion decreases with the increase in the concentration of  $\text{H}_2\text{O}$ . In the case with the exhaust gas temperature of 250 °C, the  $\text{NO}_x$  conversion yields are 48, 26, and 17% for the  $\text{H}_2\text{O}$  concentrations of 1, 5, and 10%, respectively, at the same time the values of LOT are respectively, 240, 270, and 285 °C for 1, 5, and 10% concentrations of  $\text{H}_2\text{O}$ .

This hindering behavior of  $\text{H}_2\text{O}$  could be due to the competition tendency of  $\text{H}_2\text{O}$  for taking part in the reaction with  $\text{NH}_3$  on the reaction sites of the catalyst [31].

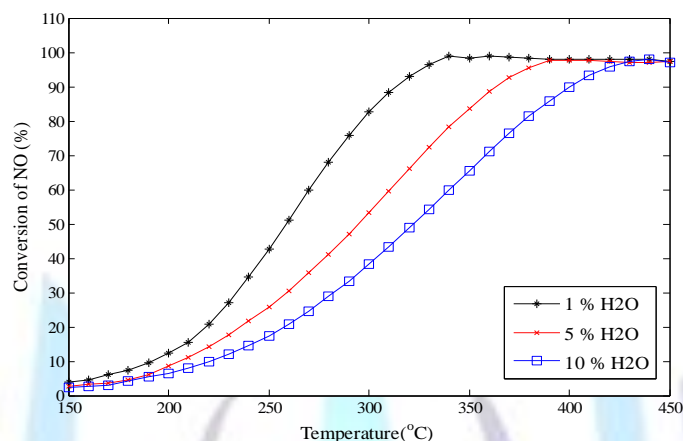


Figure 7 The effect of  $\text{H}_2\text{O}$  on NO conversion (%) under different temperature.

### 3.7 Effect of $\text{O}_2$ concentration

Exhaust gases emitted from diesel engines, generally contain  $\text{O}_2$ , whose volume is ranging from 2 to 17%, this amount of oxygen does not react with the fuel in the chamber of combustion. The results of  $\text{NO}_x$  conversion efficiency at different  $\text{O}_2$  concentrations ranging from 0.08 to 10% with the other exhaust gas conditions of 2.7%  $\text{H}_2\text{O}$ , 1000 ppm  $\text{NO}$ , 1100 ppm  $\text{NH}_3$ , and a space velocity of 8,000 [ $\text{h}^{-1}$ ] are illustrated in Fig. 8. It can be easily observed that, the  $\text{NO}_x$  conversion yield increases by temperature and approximately reaches to 98% in the temperature range of 340 and 430 °C, above this temperature, due to the oxidizing characteristics of  $\text{NH}_3$ , the efficiency shows a slight reduction. Anyway, remember that, in the temperature range mentioned here, the concentrations of  $\text{O}_2$  greater than 5% have no profound influence on the  $\text{NO}_x$  conversion. Hence, in actual diesel exhaust gases, we can conclude that the  $\text{O}_2$  concentration impact is not regarded as an crucial factor in the standard SCR reaction expressed in Eq. (1). But, in cases with the  $\text{O}_2$  concentrations lower than 5%, the  $\text{NO}_x$  conversion has shown a dramatic decrease since the standard SCR reaction can't succeed in the process of NO conversion [21].

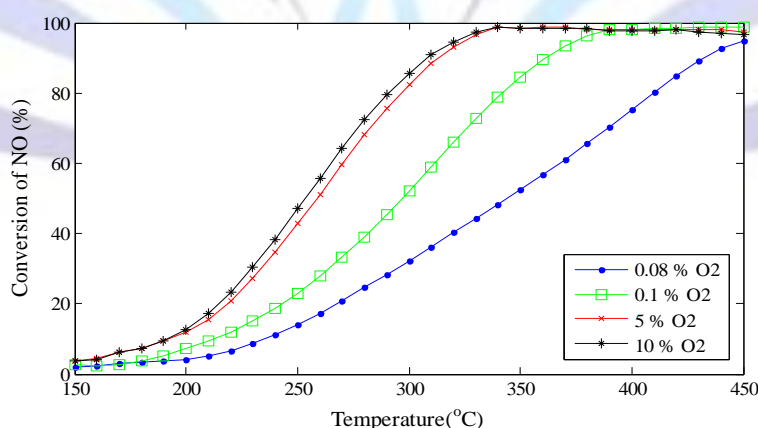


Figure 8 The effect of  $\text{O}_2$  on NO conversion (%) under different temperature.

### 3.8 The effect of cross section

After the design of the reaction mechanism and the assessment of data and examining their accordance with the experimental model, here, we discuss about the physic and the geometry of the model. First, the geometry of the SCR reactor system is designed in 3D space and then the geometrical shapes are investigated on the basis of the same geometrical coordinates defined for the part of reaction engineering software. In order to identify the desirable type of the reactor cross section, first of all, the four commonly used cross sections in this industry (including circle, hexagonal

(honeycomb) triangular and squares) are applied. The data related to the reactor stimulation and the information of each individual parts of the reactor are listed in table 1. After the application of the boundary condition of the problem and the dominant transport equations, it's the time to define the mesh of the geometry of the problem, whose related information is recorded in table 3. A scheme of a meshed reactor with a circular cross section is depicted in Fig. 2. Also, in Fig 9 the concentration profiles with different cross sections are shown. The results of the 3D model with the same size of the catalyst and equal cross sections shows a good accordance for one channel. It can be seen that the reactor with a square cross section has a greater percentage of NO conversion but the time of residence increases in the corners. The results of the comparison among the different cross sections are tabulated in table 3.

**Table 3 effect of different cross section on concentration of NO (outlet)**

Cross Section	Ratio Of Area	Concentration Of NO
Circle	1	$3.97 \times 10^{-4}$
Square	1.127	$2.56 \times 10^{-4}$
Hexagonal	1.06	$5.83 \times 10^{-4}$
Triangle	1.288	$5.56 \times 10^{-4}$

Now that we know that the reactor with a square cross section is more desirable for more reduction of NO, therefore we start to stimulate the reactor with a square shape channels. A picture of such a porous reactor is depicted in Fig 11. After meshing of the model, we discuss about the results of the stimulated reactor. In the below figure, the distribution of the nitrogen oxide in the reactor volume is illustrated. It can be observed that, in the beginning of the reactor, the reductive conversion of NO is much faster than its end. This could be due to the decrease in concentration gradient. Finally, with the help of the SCR reactor with square shape cross section, the achievement to the conversion percentages higher than 95.3% is possible.

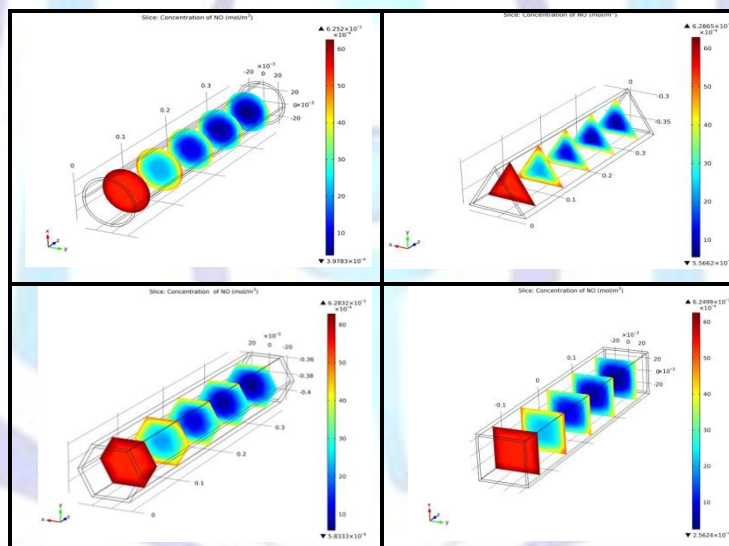


**Figure 9 comparison of concentration profile in a various cross sections of the SCR reactor.**

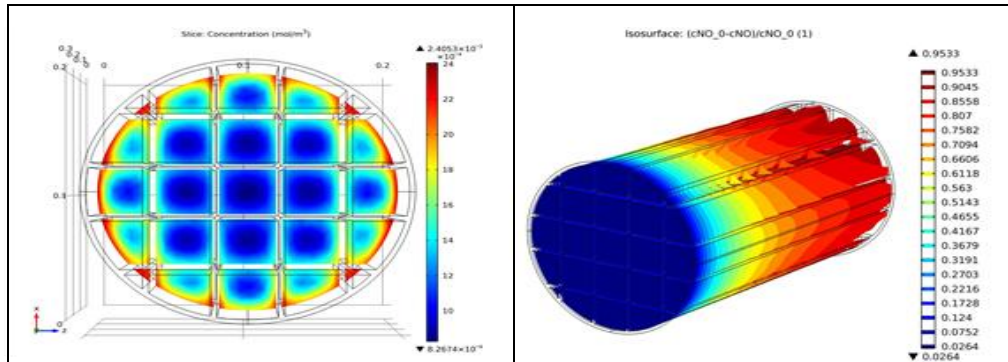


Figure 10 3D concentration plot for NO in the SCR reactor with square channel(right), at the middling section of the SCR reactor(left).

## 5 Conclusion

In order to examine the characteristics of the SCR DeNO<sub>x</sub> performance, in the presented study, a computational investigation has been made by varying the parameters such as temperature, space velocity and the O<sub>2</sub>, H<sub>2</sub>O, NO<sub>2</sub>, and NH<sub>3</sub> concentrations and also the cross section. After the introduction of the SCR model with kinetic parameters by RCGA, with the aim of the development of SCR catalysts in Diesel exhaust environments, a numerical investigation is performed on the extensive range of parameters. The possible conclusions which can be deduced from this study are as follows:

- 1) In order to make the dynamic simulation of the SCR reactor for NO reduction, the 3D mathematical model capable of describing different phenomenon such as the chemical reactions, the compressible flow of gas, the temperature-dependent viscosity and the diffusion coefficient, and the porous flow inside the catalyzed bed is introduced. The mentioned 3D dynamic model is verified and it is confirmed to be in good accordance with the experimental data. Also, for optimum search and a neural network as the decision support, a real-coded genetic algorithm model has been proposed for process optimization. It was shown that this algorithm is effective in estimation of parameters and design of the SCR reactor described by PDE model in its optimal manner. As a result, this model could be useful in enhancement of the entire examination of the effects of the key factors (such as the GHSV, operating temperature, activity energy, constant of reactions and the ratio NH<sub>3</sub>/NO) on the function of NO reduction.
- 2) The obtained results of the stimulation indicate that the NO conversion into N<sub>2</sub> is profound only when the reaction takes place in the middle range of temperature i.e. about 523k. Moreover this conclusion can be made that at the temperature of 250°C the catalytic conversion shows high effectiveness and the converter succeeded in reduction of the pollutants to a very minimum level.
- 3) Since the residence time of the exhaust gas on the surface of the catalyst would be decreased, the increase in the space velocity leads to the decrease in the performance of SCR DeNO<sub>x</sub>. Also, at temperature higher than 440 °C, the NO<sub>x</sub> conversion decreases as the oxidizing characteristics of the SCR reactions would be profound.
- 4) The concentrations of O<sub>2</sub> more than 5% does not have any dramatic influence on the conversion of NO<sub>x</sub>, anyway, in the situations with O<sub>2</sub> concentrations lower than 5%, NO<sub>x</sub> conversion dramatically decreases.
- 5) With the increase in the H<sub>2</sub>O concentration, the SCR DeNO<sub>x</sub> performance decreases. This inhibition characteristic of H<sub>2</sub>O has been explained to be the result of the competition properties of H<sub>2</sub>O with NH<sub>3</sub> on the sites of the V<sub>2</sub>O<sub>5</sub> catalyst.
- 6) As the ratio of NH<sub>3</sub>/NO<sub>x</sub> increases from 0.08 to 1.1, the performance of SCR DeNO<sub>x</sub> improves because the fast SCR reaction also takes place in the reaction of NO<sub>x</sub> conversion. However, due to the NH<sub>3</sub> inhibition behavior and oxidation effects, as the ratio of NH<sub>3</sub>/NO<sub>x</sub> exceeds the value of 1, the NO<sub>x</sub> conversion decreases.
- 7) Among the various investigated cross sections for SCR reactor for reduction of NO, the square shape cross section possesses the higher degree of conversion, about 97.7%, however, the residence time on the corners increases.

**NOMENCLATURE**

$A_i$	frequency constants, $s^{-1}$
$a$	reaction constant, $m^3 \cdot mol^{-1}$
$C_i$	concentration, $mol/m^3$
$D$	diffusion coefficient, $m^2/s$
$d_{cat}$	thickness of catalyst layer, mm
$d_{chan}$	width of channel, mm
$E_i$	activated constants, $J \cdot mol^{-1}$
GHSV	gas hourly space velocity, $h^{-1}$
$k_i$	reaction constants, $s^{-1}$
$M_i$	molar mass, $kg \cdot mol^{-1}$
$N$	number of population
$P$	pressure, pa
$R_i$	net reaction rate
$R_g$	gas constant, $J \cdot mol^{-1} \cdot K^{-1}$
$r_i$	reaction rates, $mol \cdot m^{-3} \cdot s^{-1}$
$T$	temperature, K or $^{\circ}C$
$u$	inlet velocity, $m \cdot s^{-1}$
$V$	volume of reactor, $m^3$
$X_{NO_{calc},m}$	model predicted
$X_{NO_{exp},m}$	experimental data
$\epsilon_p$	porosity of catalyst
$\rho$	density, $kg \cdot m^{-3}$
$\eta$	viscosity, $m^2 \cdot s^{-1}$
$\kappa$	permeability, $m^2$
$\sigma_i$	diameter of gas species, m
$\phi$	error function
$\Omega_D$	collision integral
$\Omega_v$	collision integral

**Subscripts**

SCR	selective catalytic reactor
g	gas
LOT	light off temperature



## REFERENCES

- [1] Soo, T.C., Dong, J.K., Young, G.K., 1997 A pilot plant study for selective catalytic reduction of NO by NH<sub>3</sub> over mordenite-type zeolite catalysts, *Catal. Today.*, **38**, 181–186 .
- [2] Lei, Z., Han, B., Yang, K., Chen, B., 2013 Influence of H<sub>2</sub>O on the low-temperature NH<sub>3</sub>-SCR of NO over V<sub>2</sub>O<sub>5</sub>/AC catalyst: An experimental and modeling study, *Chemical Engineering Journal.*, **215**, 651–657 .
- [3] Bergerson, J., Keits, D., 2005 Life cycle assessment of oil sands technologies, Institute of Sustainable Energy, *Environment and Economy, Canada.*, **11** .
- [4] Schaub, G., Unruh, D., Wang, J., Turek, T., 2003 Kinetic analysis of selective catalytic NO<sub>x</sub> reduction (SCR) in a catalytic filter, *Chemical Engineering and Processing.*, **42**, 365-371.
- [5] Kelly, J.F., Stanculescu, M., Charland, J.p., 2006 Evaluation of amines for the selective catalyst reduction (SCR) of NO<sub>x</sub> from diesel engine exhaust, *Fuel.*, **85**, 1772-1780 .
- [6] Faisal Irfan, M., Mjalli, F.S., Kim, S.D., 2012 Modeling of NH<sub>3</sub>-NO-SCR reaction over CuO/c-Al<sub>2</sub>O<sub>3</sub> catalyst in a bubbling fluidized bed reactor using artificial intelligence techniques, *Fuel.*, **93**, 245–251.
- [7] Calatayud, M., Mguig, B., Minot, C., 2004 Modeling catalytic reduction of NO by ammonia over V<sub>2</sub>O<sub>5</sub>, *Surface Science Reports.*, **55**, 169-236 .
- [8] Koebel, M., Elsener, M., 1998 Selective catalytic reduction of NO over commercial DeNO<sub>x</sub>-catalysts: experimental determination of kinetic and thermodynamic parameters, *Chem. Eng. Sci.*, **53**, 657–669 .
- [9] Economidis, N., Coil, R.F., Smiriotis, P.F., 1998 Catalytic performance of Al<sub>2</sub>O<sub>3</sub>/SiO<sub>2</sub>/TiO<sub>2</sub> loaded with V<sub>2</sub>O<sub>5</sub> for the selective catalytic reduction of NO<sub>x</sub> with ammonia, *Catalysis Today.*, **40**, 27-37 .
- [10] Kyu Yun, B., Young Kim, M., 2013 Modeling the selective catalytic reduction of NO<sub>x</sub> by ammonia over a Vanadia-based catalyst from heavy duty diesel exhaust gases, *Applied Thermal Engineering.*, **50** , 152-158 .
- [11] Ochonska-Kryca, J., Iwaniszynb, M., Piatek, M., J. Jodłowska, P., Thomasa, J., Kołodziej, A., Łojewska, J., 2013 Mass transport and kinetics in structured steel foam reactor with Cu-ZSM-5 catalyst for SCR of NO<sub>x</sub> with ammonia, *Catalysis Today.*, **216**, 135– 141 .
- [12] Zhu, Z.P., Liu, Z.Y., Niu, H.X., Liu, S.J., 1999 Promoting effect of SO<sub>2</sub> on activated carbon supported vanadia catalyst for NO reduction by NH<sub>3</sub> at low temperatures, *J. Catal.*, **187**, 245–248.
- [13] Rajadhyaksha, R.J., Hausinger, G., Zeilinger, H., Ramstetter, A., Scmelz, H., Knüzinger, H., 1989 Vanadia supported on titania—silica: Physical characterization and activity for the selective reduction on nitric oxide, *Appl. Catal.*, **51**, 67-79 .
- [14] Hadjiivanov, Klissurski, I., 1996 Surface chemistry of titania (anatase) and titania-supported catalysts, *Chem Soc. Rev.*, **25**, 61-69.
- [15] Centi, G., Perathoner, S., Biglino, P., Giamello, E., 1995 Adsorption and reactivity of NO on copper on alumina catalyst, *J. Catal.*, **152**, 75–82 .
- [16] Gieshoff, J., Sindlinger, A.S., Spurk, P.C., Van Den Tillaart, J.A.A., Garr, G., 2000 Improved SCR System for Heavy Duty Applications, *SAE.*, 2000-01-0189 .
- [17] Nam, J.G., 2007 Static characteristics of a urea-SCR system for NO<sub>x</sub> reduction in diesel engines, *International Journal Automotive Technology.*, **8** , 283-288 .
- [18] Valdes-Solis, T., Marban, G., Antonio, B.F., 2004 Kinetics and mechanism of low temperature SCR of NO<sub>x</sub> with NH<sub>3</sub> over vanadium oxide supported on carbon–ceramic cellular monoliths, *Ind. Eng. Chem. Res.*, **43**, 2349–2355.
- [19] Hsu, L.Y., Teng, H., 2001 Catalytic NO reduction with NH<sub>3</sub> over carbon modified by acid oxidation and by metal impression and its kinetic studies, *Appl. Catal. B. Environmental.*, **35**, 21–30 .
- [20] Lei, Z.G., Long, A.B., Wen, C.P., Zhang, J., Chen, B.H., 2011 Experimental and kinetic study of low temperature selective catalytic reduction of NO with NH<sub>3</sub> over the V<sub>2</sub>O<sub>5</sub>/AC catalyst, *Ind. Eng. Chem. Res.*, **50**, 5360–5368 .
- [21] Due-Hansena, J., Rasmussenc, S.B., Mikolajskac, E., Bañares, M.A, vilac, P., Fehrmanna, R., 2011 Redox behaviour of vanadium during hydrogen–oxygen exposure of the V<sub>2</sub>O<sub>5</sub>-WO<sub>3</sub>/TiO<sub>2</sub> SCR catalyst at 250 °C, *Applied Catalysis B: Environmental.*, **107**, 340– 346.
- [22] Chen, C.T., Tan W.L., 2012 Mathematical modeling, optimal design and control of an SCR reactor for NO<sub>x</sub> removal, *Taiwan Institute of Chemical Engineers.*, **43**, 409–419 .
- [23] Dhanushkodi, SR., Mahinpey, N., Wilson, M., 2008 Kinetic and 2D reactor modeling for simulation of the catalytic reduction of NO<sub>x</sub> in the monolith honeycomb reactor , *Process Safety and Environment Protection.*, **86**, 303–309 .
- [24] Tronconi, E., Forzatti, P., Martin, J.P.G., Mallogi, S., 1992 Selective catalytic removal of NO<sub>x</sub>: a mathematical model for design of catalyst and reactor, *Chemical Engineering Science.*, **47**, 2401–2406 .



- [25] Chuang, YC., Chen, CT., A., 2011 study on real-coded genetic algorithm for process optimization using ranking selection, direction-based crossover and dynamic mutation, *IEEE Congress on Evolution Computation.*, **160**, June 5–8 .
- [26] Saracco, G., Specchia, V., 1998 Catalytic filter for flue gas cleaning, in: Cybulski, A., Moulijn, J.A., (eds.), *Structured Catalysts and Reactors.*, pp, 417-434 .
- [27] Turek, T., 1992 Katalytische Reduktion von Stickstoffmonoxid in einem rotierenden Wa"rmeu" bertrager, *Dissertation, Universita"t Karlsruhe* .
- [28] Liu, F., He, H., Zhang, C., Zhang, F., Zhang, L., Xie, Y., Hu, T., 2010 Selective catalytic reduction of NO with NH<sub>3</sub> over iron titanate catalyst: catalytic performance and characterization, *Applied Catalyst B: Environmental.*, **96**, 408-420 .
- [29] Yang, T.T., Bi, H.T., Cheng, X., 2011 Effect of O<sub>2</sub>, CO<sub>2</sub>, and H<sub>2</sub>O on NO adsorption and selective catalytic reduction over Fe/ZSM-5, *Applied Catalyst B: Environmental.*, **102**, 163-171 .
- [30] Willi, R., Roduit, B., Koepfel, R.A., Wokaun, A., Baiker, A., 1996 Selective reduction of NO by NH<sub>3</sub> over Vanadia based commercial catalyst: parametric sensitivity and kinetic modeling, *Chemical Engineering Science.*, **51**, 2897-2902 .
- [31] Busca, G., Lietti, L., Ramis, G., Berti, F., 1998 Chemical and mechanistic aspects of the selective catalytic reduction of NO<sub>x</sub> by ammonia over oxide catalysts: a review, *Applied Catalysis B: Environmental.*, **18**, 1-36 .

